Production of Li and B in proton and alpha-particle reactions on ^{14}N at low energies*

W. W. Jacobs,† D. Bodansky, D. Chamberlin, and D. L. Oberg
Department of Physics, University of Washington, Seattle, Washington 98195
(Received 28 January 1974)

Cross sections have been measured for the production of ^{7}Li and ^{11}B from the reactions $^{14}N(p,2\alpha)^{7}Be$ and $^{14}N(p,\alpha)^{11}C$ from near threshold to 24 and 22 MeV, respectively, and for the production of ^{6}Li and ^{10}B in α-particle bombardment of ^{14}N up to 42 MeV. The proton reactions were studied with activation techniques and the α-particle reactions investigated using time-of-flight particle identification. These cross sections are of interest because of their relevance to the production of the light elements in nature by relatively low-energy particles. Analyses of comparative production cross sections from CNO targets indicate that it is possible to match the solar system abundances of LiBeB with reactions dominated by protons of energies below about 25 MeV, provided one accepts the higher of recent estimates of the B abundance.

[NUCLEAR REACTIONS $^{14}N(p,2\alpha)$, $E=14-24$ MeV; $^{14}N(p,\alpha)$, $E=5-22$ MeV; $^{14}N(\alpha,^{10}B)$, $^{14}N(\alpha,^{6}Li)$, $E=21-42$ MeV; measured $\sigma(E)$. Astrophysical production of Li and B.]

I. INTRODUCTION

It is generally assumed that the light elements, Li, Be, and B, are by-passed in the main chain of stellar nucleosynthesis, because they are readily destroyed in exoergic (p, α) reactions at hydrogen burning temperatures. A wide variety of alternative mechanisms have been suggested for light element production, primarily involving the breakup of C, N, and O, through endoergic reactions with protons and α particles. Proposed processes include reactions in active regions near the stellar surface,[1,2] reactions between galactic cosmic rays and nuclei in interstellar space,[3-6] and reactions in supernova shock waves.[7-9] In some of these analyses it has been concluded that insufficient ^{7}Li will be produced to match observed solar system abundances, and therefore special mechanisms have been invoked for ^{7}Li production, including big-bang nucleosynthesis,[10] and stellar synthesis by the $^{3}He(\alpha,\gamma)^{7}Be$ reaction with rapid mixing to cool regions.[11] Broad surveys dealing with light element production have been presented by Truran and Cameron,[12] Mitler,[5] Reeves, Audouze, Fowler, and Schramm,[6] and Reeves.[13]

The present work[14] is concerned with cross sections for the production of light elements in proton and α-particle interactions with ^{14}N. The proton thresholds for light element production are much lower for ^{14}N than for ^{12}C or ^{16}O.[2] In particular, ^{7}Li and ^{11}B are produced through the $^{14}N(p, 2\alpha)^{7}Be$ and $^{14}N(p, \alpha)^{11}C$ reactions with thresholds at 11.21 and 3.13 MeV, respectively. If the proton flux in the neighborhood of 10 or 20 MeV is much greater than at higher energies, then the ^{14}N reactions dominate ^{7}Li and ^{11}B production. We have measured the excitation functions for these reactions from near threshold to about 22 MeV using activation techniques. The present results can be compared to previous measurements for protons on ^{14}N by Epherre and Seide[15] and by Laumer, Austin, Panggabean, and Davids.[16]

The abundance of α particles, in the cosmic ray flux (expressed in energy per nucleon) or as a target, is of the order of 10% that of protons, and therefore it might be expected that α particles would play relatively little role in the synthesis of the light elements. However, as projectiles they have very low reaction thresholds, again if expressed in MeV per nucleon, and for incident CNO nuclei of given energy the c.m. energy will be much greater for ^{4}He than for ^{1}H targets. Thus, if the incident spectra are rising rapidly at low energies, α-particle reactions will be enhanced. The α-particle reactions with lowest thresholds are those for the production of ^{6}Li and ^{10}B in interactions with ^{14}N, with thresholds at 2.83 and 3.73 MeV per nucleon, respectively. We have measured the cross sections for these reactions at incident energies extending from 21 to 42 MeV, using time-of-flight techniques to identify the reaction products of interest.

The proton measurements and the low-energy α-particle measurements were carried out using the University of Washington three-stage tandem Van de Graaff accelerator, while the α-particle

measurements at higher energies were performed with the University of Washington 60-in. cyclotron. Problems of target preparation and normalization, common to all the measurements, are described in Sec. II. The experimental procedures and cross-section results for the reaction $^{14}N(p, \alpha)^{11}C$, for the reaction $^{14}N(p, 2\alpha)^{7}Be$, and for the various α-particle induced reactions leading to the production of ^{6}Li and ^{10}B are described in Secs. III, IV, and V, respectively. The implications of these results are discussed briefly in Sec. VI.

II. TARGETS AND NORMALIZATION PROCEDURES

The nitrogen targets were made by evaporating adenine ($C_5H_5N_5$) onto backing foils of aluminum or carbon. For the proton activation runs the target was composed of two foils in an aluminum-adenine-aluminum sandwich. The aluminum backing foils served as catchers for the radioactive products of interest, and had thicknesses ranging from about 1.4 to 7 mg/cm^2. The total adenine thickness for each target was in the neighborhood of 1–2 mg/cm^2. These relatively large adenine thicknesses were helpful in reducing the data collection time, and, as discussed further in Sec. III, made it easier to avoid gaps in the excitation function for the $^{14}N(p, \alpha)^{11}C$ reaction. The adenine surfaces were each coated with a polystyrene film, approximately 0.1 mg/cm^2 thick, to increase the stability of the targets against physical damage, such as flaking. For the α-particle induced reactions, where the outgoing reaction products themselves were observed, thinner targets were used, ~100-μg/cm^2 adenine evaporated onto 25-μg/cm^2 carbon foils. For these targets it was found that there was no need for a protective polystyrene film.

For purposes of normalization a spectrum of scattered particles was collected during each data run using a solid state monitor detector. The product Φt of the beam flux Φ and the target thickness t was calculated from the number of counts in the ^{14}N elastic peak, the detector solid angle, and the separately determined ^{14}N elastic scattering cross section.

The elastic scattering cross sections were determined in measurements using a gas target[17] and a Faraday cup for beam flux determination. The gas cell was cylindrical, approximately 7.6 cm high and 3.8 cm in diameter, with 2.5-μm Havar entrance and exit foils, oriented with the target axis normal to the reaction plane. The target was viewed by a solid state detector using a two-slit aperture system and the cross section was calculated from a standard expression relating the cross section to the observed counts, the gas density, and the aperture geometry.[18] The cross sections were determined to within an estimated uncertainty of about 4%, with the largest individual uncertainty being in the aperture geometry. In order to check the accuracy of the gas target measurements, the $^{1}H(p,p)^{1}H$ cross section was measured at 9.918 MeV and the results compared to those determined by Jarmie *et al.*[19] The measured values for different runs agreed with the Jarmie values to within 3.5%, and the ratio of the two results was applied as a correction to the ^{14}N elastic cross sections, slightly reducing their over-all uncertainty. For proton energies below 10 MeV, data were taken at frequent energy intervals and with thick gas targets, in a manner to match the energy intervals defined by the adenine target thickness. At higher proton energies and for the α particles, no attempt was made to match the adenine target energy intervals.

It was possible, although not necessary for the analysis of the data, to determine the adenine target thickness and stability using the measured number of monitor counts, the elastic cross section, and the beam flux. The thicknesses obtained in this manner usually agreed within 10% with the thicknesses found from weighing the targets after their initial preparation, indicating that the targets were uniform and stable. In general, the thick targets withstood proton beam intensities below about 40 nA, while the thinner targets used in the α-particle runs showed no deterioration with α-particle currents up to 50 nA.

III. DETERMINATION OF THE $^{14}N(p,\alpha)^{11}C$ CROSS SECTIONS

For the $^{14}N(p, \alpha)^{11}C$ cross-section measurements, the adenine targets were activated in 5-min bombardments, and were counted over a period typically in the neighborhood of 100 min. The normalization factor Φt was determined during the bombardment, using the monitor detector as discussed in Sec. II. In addition, counts from the monitor were recorded at 1-min intervals during the irradiation, and corrections made for variations in the incident beam intensity. The cross sections were calculated from the relation $\sigma = A_0/\epsilon\lambda\Phi t$, where A_0 is the detected activity extrapolated to zero time, ϵ is the detector efficiency, and λ is the decay constant.

The target activity was determined by coincidence counting of the annihilation γ rays from the 20.34-min positron decay of ^{11}C. Two 7.6×7.6-cm NaI(Tl) crystals were used, 28 cm apart, with the target placed midway between them. In order to stop the positrons from ^{11}C (endpoint energy = 0.96 MeV), 2.4-mm-thick aluminum discs were placed against each side of the target. The efficiency ϵ

for the detection of the annihilation radiation from ^{11}C decay was 0.0068 ± 0.0004, as determined by comparison with a ^{22}Na calibration source (positron endpoint energy = 0.54 MeV), including corrections for the loss due to interactions of the 511-keV γ rays in the aluminum discs, and the larger effective source size for the ^{11}C activity.

In addition to the 20.34-min activity from ^{11}C, the decay curve contains a 9.96-min component from ^{13}N, produced with low yield at all energies by the $^{12}C(p, \gamma)^{13}N$ reaction and with high yield above its 9.96-MeV threshold by the $^{14}N(p, d)^{13}N$ reaction. The observed decay curve was matched with a three-component computer fit, including the 20.34-min ^{11}C and 9.96-min ^{13}N components as well as a 109.7-min component which might arise from the $^{18}O(p, n)^{18}F$ reaction in an oxygen target impurity. In fact, however, there was no evidence of a 109.7-min half-life and the term was retained in large part as a means of accounting for all long-lived contributions, including room background. The calculated 9.96-min component varied from being negligible at very low energies to accounting for nearly 50% of the extrapolated activity at the higher energies. The calculated 109.7-min component was much smaller, and its omission from the fitting program typically changed the extrapolated ^{11}C activity by only 2%. The over-all uncertainty in the initial ^{11}C activity arising from uncertainties in the fitting of the decay curve was estimated to be 3%.

Previous investigations have shown that a significant amount of the ^{11}C activity produced in the bombardment of polyethylene and polystyrene targets may be lost through the escape of radioactive gases,[20] with the losses for polyethylene being more than twice as great as those for polystyrene. The possible loss of activity from adenine targets was investigated by bombarding typical targets within a special vacuum tight cell, counting the annihilation radiation for approximately 45 min, flushing the cell with helium, and then resuming counting. Presumably the flushing would remove any gas which diffuses from the target, and the loss of gas would appear as a break in the decay curve. No such break was seen in repeated tests with adenine targets, although a 4.5% shift was seen with a 9.9-mg/cm^2 polyethylene target. This loss was about a factor of 3 less than seen for polyethylene by other authors.[20] In the absence of an explanation for our relatively low value for the loss of activity from polyethylene, the experimental upper limit of 1% was replaced by an assumed upper limit of 3% for the loss of ^{11}C from the adenine targets.

A special problem arose at points above 18 MeV, because of the onset of the $^{12}C(p, d)^{11}C$ reaction, with a threshold at 17.87 MeV. To correct for ^{11}C activity from this reaction, separate runs were taken with a polyethylene target. The activity attributable to the carbon in the adenine targets was then inferred by using a relative normalization based on the size of the carbon elastic peaks seen in the monitor detector and was subtracted from the total ^{11}C adenine activity. Uncertainties arising from this subtraction, including those associated with gas loss from the polyethylene, make the errors above 18 MeV much greater than at lower energies.

The measured cross sections for the $^{14}N(p, \alpha)^{11}C$ reaction are displayed in Fig. 1, along with results obtained by previous investigators. The region from 5 to 15 MeV was covered in 100-keV steps, and the region above 15 MeV in 1-MeV steps. Each data point represents a cross section averaged over an incident energy interval determined by the target thickness. At the lower energies, this interval was purposely made large, to avoid missing possible contributions from sharp peaks in the excitation function. Up to 10.5 MeV, the effective target thickness was kept at 120 keV by the selection of the targets and by adjustment of the target angle. Thus the points here are over-

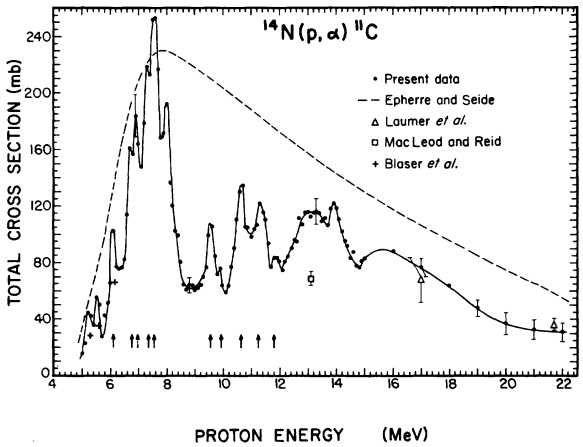

FIG. 1. Total cross section for the $^{14}N(p,\alpha)^{11}C$ reaction as a function of proton energy. The solid line through the data points is to guide the eye. Sample error bars below 18 MeV correspond to an absolute uncertainty of 8.5%. Above 18 MeV, the errors range from 8.5 to 20%, as indicated. Cross sections reported by other authors are also plotted: Epherre and Seide (Ref. 15), Laumer *et al.* (Ref. 16), MacLeod and Reid [Proc. Phys. Soc. Lond. 87, 437 (1966)], and Blaser, Marmier, and Sempert [Helv. Phys. Acta 25, 442 (1952)]. The arrows at the lower energies indicate the positions of resonances interpreted as resulting from α-^{11}C core coupling.

lapping. From 10.5 to 15 Mev, because of the lesser stopping power and a limit to the practical target thicknesses, the effective target thicknesses were smaller, ranging from 60 to 90 keV. However, it is unlikely that any significant peaks in the excitation function were missed. Above 10 MeV there is no evidence in the data of resonances narrower than 100 keV; the expected level width at ^{15}O excitation energies near 17 MeV (corresponding to 10.5-MeV protons) is about 150 keV,[21] and the widths for those resonances in ^{14}N+p above $E_p = 7$ MeV for which Γ has been previously determined are all well above 100 keV.[22] Above 15 MeV no attempt was made to avoid gaps in the excitation function, and the targets were typically 20 to 35 keV thick. Thus there is some chance that peaks at intermediate points in this part of the excitation function were missed, although the smooth appearance of the measured data gives no suggestion of structure. It is not likely that there is any substantial variation in the cross section at high energies due to Ericson fluctuations because of the averaging effect for total cross sections, and because the ^{11}C yield involves the summation over α-particle transitions to a number of states of ^{11}C.

Up to 18 MeV the estimated uncertainty in the absolute cross sections is 9%. This uncertainty arises in large measure from the 5% uncertainty in the absolute calibration of the annihilation radiation detector. Further appreciable contributions, each about 3%, come from the decay curve analysis, the determination of the number of counts in the monitor peak, the determination of the normalization cross section, and possible loss of ^{11}C from the target. Above 19 MeV, the absolute uncertainty is approximately 20%, the additional uncertainty arising from the activity produced in the ^{12}C(p, d)^{11}C reaction. Within these uncertainties the present results are in good agreement with those of Laumer *et al.*[16] displayed in Fig. 1, but are not in agreement with the results of Epherre and Seide,[15] obtained by making integral activation measurements on targets of vanadium nitride. The latter authors estimate their uncertainties to be 20 to 25%, but in some regions the discrepancies appear to exceed the combined quoted uncertainties.

The strong structures indicated by arrows in the excitation function of Fig. 1 below 12 MeV match resonances in ^{15}O which have been previously seen in (p, p') and (p, α) studies on ^{14}N, and which have been interpreted in terms of α-particle states built upon a ^{11}C core.[23] Most other low-energy structures can be identified with observed resonances in the ^{15}O compound system,[22] and the larger structures above 12 MeV may result from further, as yet unidentified, α-^{11}C core couplings.

IV. DETERMINATION OF THE ^{14}N(p,2α)^{7}Be CROSS SECTIONS

In the ^{14}N(p, 2α)^{7}Be measurements, the adenine targets were bombarded for about 2 h. Counting of the targets was begun a week or two after the bombardments and continued for about 100 days. The normalization procedures and the cross section calculations were carried out as described in Sec. III.

The target activity was determined by counting 478-keV γ rays from the decay of the first excited state of ^{7}Li. This state is formed by electron capture in ^{7}Be with a branching ratio[24] of (10.32 ± 0.16)%. The γ rays were detected in a 7.6×7.6-cm NaI(Tl) detector, usually at a target-to-detector distance of 5 or 10 cm. There was no indication in the NaI spectra of contributions from unresolved lines, such as 511-keV annihilation ra-

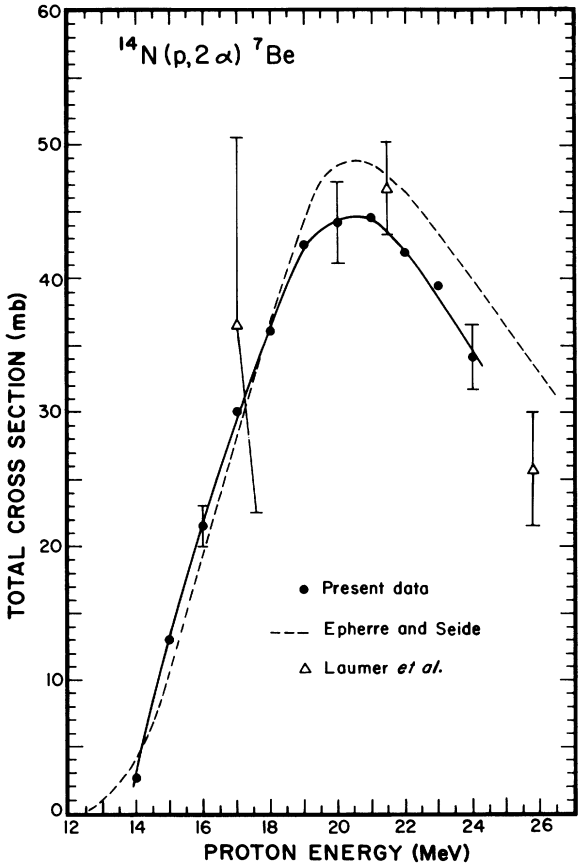

FIG. 2. Total cross section for the ^{14}N(p, 2α)^{7}Be reaction as a function of proton energy. The solid line through the present data points is to guide the eye. The indicated error bars correspond to an absolute uncertainty of 7.5%. Cross sections reported by other authors are also plotted: Epherre and Seide (Ref. 15) and Laumer *et al.* (Ref. 16).

diation, as confirmed by auxiliary tests with a Ge(Li) detector.

The efficiency of the NaI detector was determined from measurements with an array of calibration sources which bracketed 478 keV. The measured efficiencies were in good agreement with values calculated by Heath,[25] and the 478-keV efficiency was therefore taken to be the Heath calculated value, modified by a correction of 0.4 to 2.3% (depending upon distance) to account for small systematic discrepancies between the Heath values and the measured values. The resulting efficiencies at 5 and 10 cm were 0.0399 ± 0.0019 and 0.0145 ± 0.0007, respectively.

The measured decay curve was well matched by the half-life of ^{7}Be, taken here to be 53.6 days; no other decay component was suspected or observed. The resulting cross sections for incident proton energies from 14 to 24 MeV are plotted in Fig. 2. The absolute uncertainty at each point is about 7.5%, and arises primarily from uncertainties of 5% in determining the normalization factor Φt and 5% in the NaI(Tl) detector efficiency determination. The present results are seen to be in good agreement with the results of Epherre and Seide,[15] who quote absolute uncertainties of 17%, and the results of Laumer *et al.*[16]

V. DETERMINATION OF CROSS SECTIONS WITH INCIDENT α PARTICLES

The products of interest in the α-particle bombardments of ^{14}N were ^{6}Li and ^{10}B. While other heavy ions are energetically possible, ^{6}Li and ^{10}B have the lowest production thresholds by a considerable margin, and are formed through reactions which are expected to have high cross sections. It is presumed that ^{10}B is produced primarily in the $(\alpha, 2\alpha)$ reaction, with some contribution from $(\alpha, {}^{8}\mathrm{Be})$. At the lowest incident energies ^{6}Li is produced through the reaction $^{14}\mathrm{N}(\alpha, {}^{12}\mathrm{C})^{6}\mathrm{Li}$, but above the $^{14}\mathrm{N}(\alpha, 3\alpha)^{6}\mathrm{Li}$ threshold at 20.7 MeV, a major contribution is presumed to come from events proceeding through excited states of ^{10}B which decay by α-particle emission. Knowledge of the specific channels is not essential to the determination of the total yields of ^{6}Li and ^{10}B and no attempt was made to experimentally identify the reaction channels, except in cases of well defined transitions to discrete states of the product nuclei.

Measurements were made at incident α-particle energies of 21, 23, 25, and 26 MeV using the tandem Van de Graaff accelerator and at 31.5, 34.4, and 42.1 MeV using the cyclotron. The lower cyclotron energies were obtained by degrading the 42-MeV α-particle beam with beryllium foils placed 24 cm in front of the target. Apertures between the degrader and target intercepted those particles which were scattered through angles large enough to miss either the target or the Faraday cup.

The basic experimental arrangement was the same for the Van de Graaff and cyclotron runs. In each case, time-of-flight particle identification was carried out using two independent solid state detector telescopes situated 10° apart in a 152-cm-diam scattering chamber. Each telescope consisted of a surface barrier detector, 300 mm^2 by 200 μm, followed by a lithium-drifted silicon detector, 350–400 mm^2 by 2000 μm. All ^{6}Li and heavier ions stopped in the first detector; the second detector was used for anticoincidence rejection of high-energy α particles and lighter ions. A 1.75-cm aperture in front of the detectors defined the solid angle. The flight path from the target to the front detector was kept at 64 cm for all runs.

The particle energy was determined from an amplified linear signal from the front detector. The flight time was established by starting a time-to-amplitude-converter (TAC) with a fast signal from the front detector and stopping it with a signal from the accelerator. In the case of the Van de Graaff, the beam was chopped and bunched at low energies, and the stop signal came from the buncher oscillator. For the cyclotron the natural bunching of the beam was used, and the stop signal came from the cyclotron oscillator. The beam bunch widths at the targets were typically 2.5 nsec full width at half-maximum (FWHM) for the Van de Graaff and about 1 nsec (FWHM) for the cyclotron. The period between bunches for the cyclotron was only 87 nsec, and to avoid overlap between slow particles from one bunch and fast particles from the next bunch it was necessary to reject ^{6}Li ions below 2 MeV and ^{10}B ions below 3 MeV. There was no comparable limitation for the Van de Graaff runs, where the repetition period was about 330 nsec; the low-energy threshold of about 0.5 to 0.8 MeV was determined by the detector system.

The energy signal E and the TAC output T' for each telescope were fed to the input analog-to-digital converters of an on-line XDS-930 computer. The computer was gated by pulse height windows on each of the signals, as well as by the requirement of no signal from the anticoincidence detector. Mass identification was accomplished within the computer, using the algorithm $M = C(E - E_0) \times (T_0 - T')^2$, where C is a proportionality constant, E_0 a small correction term to compensate for nonlinearities at low energies, and T_0 is a parameter used to transform the TAC conversion time T' to the actual flight time, $T = T_0 - T'$. The several

parameters were established empirically to develop a two-dimensional display of mass vs particle energy, in which particles of the same mass fall in a horizontal band. The basic data of the measurements were the number of counts at each point of this two-dimensional mass-energy array. The separation between the mass bands was not complete, and for both the ^{6}Li and ^{10}B bands it was necessary to make subtractions for tails from neighboring mass groups. The magnitude of the subtraction varied from 5 to 60% of the total number of counts in each energy channel, leading to net uncertainties from the subtraction estimated to range between 1 and 12%.

At the Van de Graaff energies, 26 MeV and lower, the only clearly defined ^{6}Li events were for discrete groups corresponding to leaving ^{12}C in its ground or 4.43-MeV excited states. At the cyclotron energies, 31.5 MeV and above, the ^{6}Li yield was dominated by contributions from the continuum, although both bound and unbound excited states of ^{12}C were identifiable. The ^{10}B spectrum was in all cases dominated by continuum events, although in many runs a discrete group corresponding to leaving ^{8}Be in its ground state was visible. ^{10}B spectra taken at 26 MeV are illustrated in Fig. 3.

The total cross sections for the ^{12}C(g.s.) and ^{12}C(4.43) ^{6}Li groups were found at each energy by integration of the c.m. differential cross section. In the best data, angular distributions were obtained in 10° steps from 10 to 170°(lab), and the extrapolation to the unmeasured angular interval introduced negligible error. However, at some of the energies, and particularly for the 4.43-MeV group, the data were more limited, with the solid angle for the unobserved region amounting to between 10 and 25% of the full solid angle. Here the estimated uncertainties in the extrapolation were from 5 to 15% of the total cross section. At 21 MeV, however, as much as 60% of the c.m. solid angle was missed, and a crude extrapolation was made by assuming that the actual 21-MeV angular distributions were the same as the average of the angular distributions at 23 and 26 MeV. An uncertainty of 40% was arbitrarily assigned to the 21-MeV cross sections thus obtained.

For the continuum region, yields for identifiable final states [such as ^{6}Li + ^{12}C(7.65) or ^{10}B + ^{8}Be (g.s.)] were separately extracted and the corresponding total cross sections calculated. These generally amounted to less than 5% of the total continuum region yield. For the remainder of the continuum region events, the c.m. differential cross section was calculated for each (lab) energy channel, and the results regrouped to synthesize

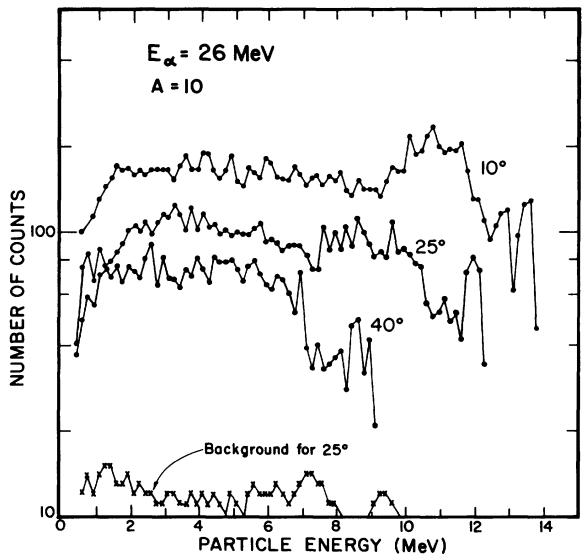

FIG. 3. ^{10}B energy spectra (lab) for the ^{14}N(α,2α)^{10}B reaction at 26 MeV, at several angles. The background contribution from adjacent mass groups is shown for the 25° spectrum. Peaks corresponding to the ^{8}Be ground state can be seen in the spectra at the highest energies.

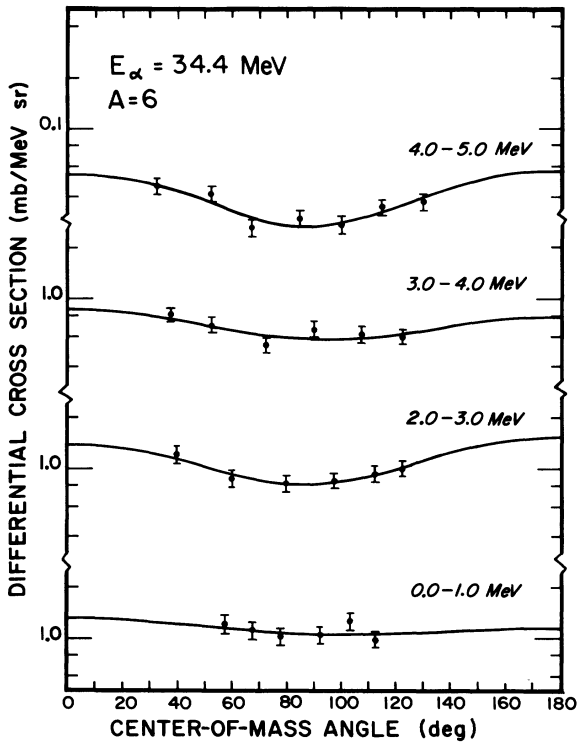

FIG. 4. ^{6}Li angular distributions (c.m.) for continuum events in the 34.4-MeV α-particle bombardment of ^{14}N. The data have been averaged over a c.m. energy bin of 1 MeV, as indicated. The error bars represent estimated total uncertainties. The curves are best fits to the data of the function $A + B\cos\theta + C\cos^2\theta$.

angular distributions for fixed c.m. energy bins. The data on which these distributions were based extend to values of c.m. energy which, at angles near 90° (c.m.), are much below the magnitudes of the laboratory energy thresholds. A typical set of angular distributions is shown in Fig. 4, where the laboratory threshold was 2 MeV, but the distributions include points at c.m. energies below 0.4 MeV. Thus conversion to the c.m. in effect replaces a laboratory energy extrapolation by a c.m. angular extrapolation.

Although the laboratory distributions are strongly forward peaked, with no internal guides toward the proper shape of the extrapolation to unmeasured regions, the c.m. distributions are seen to be moderately flat and almost symmetric about 90°, as would be expected for distributions representing averages over many compound nuclear channels. These distributions were fitted with a sum of Legendre polynomials extending to $P_2(\cos\theta)$. The even terms give a distribution symmetric about 90°, of the form $A+B\cos^2\theta$, while the $P_1(\cos\theta)$ term allows for possible forward or backward peaking. It is seen that the asymmetry is rather slight, and that the distributions become flatter at lower outgoing particle energies. These were general features of both the ^{6}Li and ^{10}B continuum distributions. Because the use of the three-term Legendre polynomial fit represented a conjecture, rather than a well substantiated model, it was assumed that there was an uncertainty in the extrapolation corresponding to $\frac{1}{3}$ of the fraction of the c.m. solid angle which was unmeasured. This led to an additional error in the total cross section, typically in the neighborhood of 10%.

The resulting excitation functions for the production of ^{6}Li and ^{10}B in α-particle bombardment of ^{14}N are plotted in Figs. 5 and 6. In the former case the yields for the ^{12}C ground state, the ^{12}C

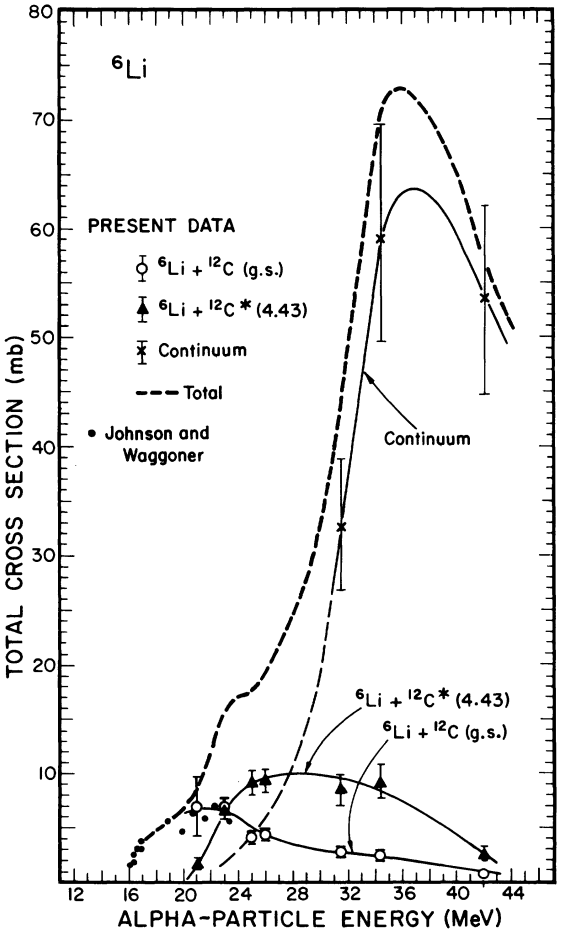

FIG. 5. Cross sections for the production of ^{6}Li in the α-particle bombardment of ^{14}N as a function of α-particle energy. Separate plots are given for cross sections for the bound states of ^{12}C, for the 3α continuum region, and for the sum. The curves through the data points are to guide the eye, and for the continuum and total cross sections are qualitatively speculative. Cross sections for the ^{12}C ground state determined from the ^{12}C(^{6}Li, α)^{14}N measurements of Johnson and Waggoner (Ref. 26) are also shown.

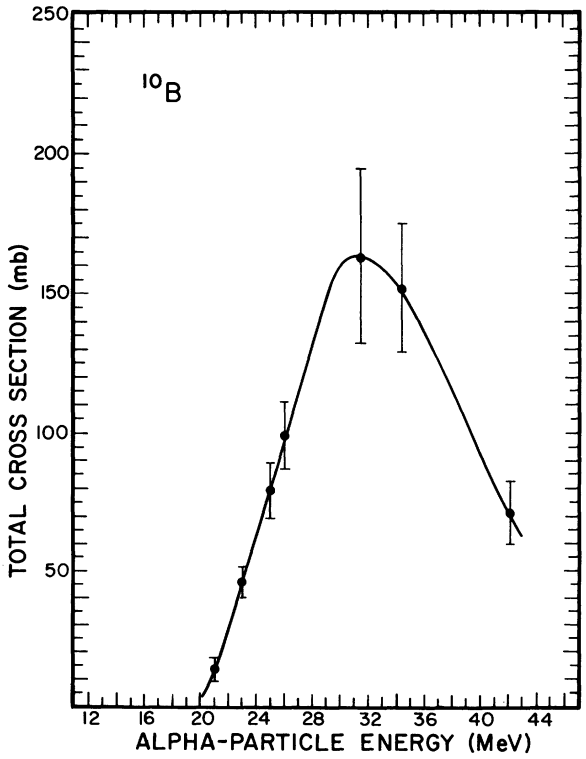

FIG. 6. Total cross section for the production of ^{10}B in the α-particle bombardment of ^{14}N as a function of α-particle energy. The curve through the data points is to guide the eye.

4.43-MeV state, and the continuum region are plotted separately, together with the combined total yield. The continuum region results include both the true continuum and the superposed discrete states. Over-all errors in the cross sections are indicated for each point. For the continuum region, which provides the largest cross sections, they range from 16 to 19%, except for the ^{10}B results at 21 MeV, where the uncertainty is 25%. These errors include the statistical uncertainties, extrapolation uncertainties, and uncertainties in the target thickness and background subtraction.

The ^{12}C ground-state results can be compared, through detailed balance, with the measurements of Johnson and Waggoner[26] for the ^{12}C(Li, α)^{14}N cross section. Although in the region of overlap the errors in the present data are large, there is agreement within these errors, and the data of Johnson and Waggoner can serve to extend the total cross-section results to lower energies than found in the present measurements themselves.

VI. DISCUSSION

Ultimately cross sections such as those presented above should be incorporated in a model for light element production which specifies definite production mechanisms and environments, including energy spectra and initial abundances for the interacting nuclei, and in which all reactions leading to element production and destruction are followed. Calculations of this sort, bearing on light element production, have, for example, been carried out for a galactic cosmic-ray model by Meneguzzi, Audouze, and Reeves,[4] for a big-bang model by Wagoner,[10] and for supernova explosions by Epstein, Schramm, and Arnett.[27]

Here we investigate a more limited question: Do the cross sections for proton reactions with the CNO nuclei in themselves rule out the possibility that the light elements are produced chiefly in reactions at low energy, up to several tens of MeV? This supposition is incompatible with versions of galactic cosmic-ray production models in which the cosmic-ray spectrum is described by a power law in total energy. However, it could be consistent with less restrictive galactic cosmic-ray models, as well as with production in supernova, big bangs, or stellar flares.

The possible role of low-energy particles was discussed by Bernas, Gradsztajn, Reeves, and Schatzman[2] and has been considered to a limited extent by subsequent authors.[28] Bernas *et al.* pointed out the crucial role of ^{14}N at low energies, as well as the fact that little experimental data on ^{14}N cross sections were then available. A major difficulty, as they indicated, was the apparent excessive production of B at low energies. Subsequent cross-section measurements now make possible a more quantitative examination of such a description, and the problem with the B/Li ratio may have been removed by the suggestion of Cameron, Colgate, and Grossman[7] (hereafter referred to as CCG) that the B abundances have previously been seriously underestimated. However, recent measurements by Morton *et al.*[29] showed no interstellar B II absorption lines in the direction of Xi Persei, and these results have been interpreted by Audouze, Lequeux, and Reeves[30] as implying an upper limit for the cosmic B/H ratio of 2×10^{-9}, which is about $\frac{1}{5}$ that of the CCG analysis. On the other hand, Boesgaard and Heacox[31] have found a B/H ratio of 1.9×10^{-7} in observations of Kappa Cancri, and interpret this as requiring light element production processes which give high B yields. At present, the question of the relative B and Li cosmic abundances appears to be unsettled, and we will here explore consequences of accepting the CCG value.

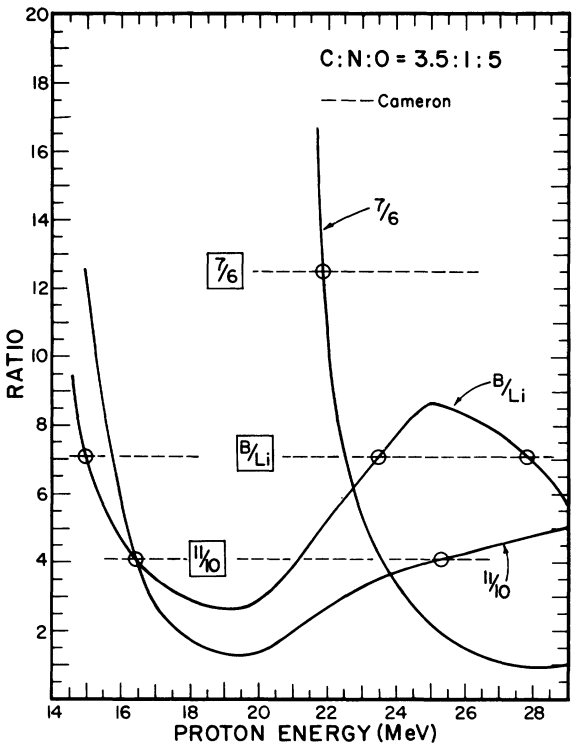

FIG. 7. Ratios of the 7/6, 11/10, and B/Li yields for proton reactions with C, N, and O in a representative target abundance mixture. The horizontal lines correspond to the ratios for the Cameron solar system abundances (Ref. 32). Proton energies where the calculated ratios match the given solar system ratios are indicated by circles.

In Fig. 7 a comparison is made between observed ratios of ^{7}Li/^{6}Li, ^{11}B/^{10}B, and B/Li, based on the solar system abundances tabulated by Cameron,[32] and ratios calculated at given energy for light element production in proton bombardment of CNO nuclei. The abundances of C, N, and O are assumed to be in the ratios of 3.5 : 1 : 5, in a crude approximation to the solar system ratios[32] of 3.2 : 1 : 5.8 and to observed galactic cosmic-ray ratios[33] of 3.9 : 1 : 3.6. Cross sections for ^{14}N-$(p, \alpha)^{11}$C and ^{14}N$(p, 2\alpha)^7$Be are taken from the present work for energies up to 22 and 24 MeV, respectively, and the remaining cross sections are taken from the extensive investigations by the Michigan State group.[16,34,35] It should be noted that below 30 MeV ^{16}O plays almost no part, and that, except for the production of ^{11}B above 20 MeV, the ^{12}C cross sections are small (although not negligible) compared to the ^{14}N cross sections.

As seen in Fig. 7, the Cameron B/Li and 11/10 ratios are matched by the calculated production yields at several energies between 15 and 28 MeV, and it is clear that they could be accounted for by a variety of proton energy distributions in the region below 30 MeV. The solar system 7/6 ratio is matched only near 22 MeV, but some properly weighted distribution in the vicinity of 20 to 25 MeV could duplicate the observed ratio. All the ratios are rising toward the lower energies where the yields are dominated by the ^{14}N$(p, \alpha)^{11}$C reaction and, to a lesser extent, by the ^{14}N$(p, 2\alpha)^7$Be reaction. If the relative ^{13}C abundance is greater than the solar system value, there will be significant contributions to the production of ^{10}B and ^{6}Li from ^{13}C reactions,[36] permitting fits at lower proton energies, but this possibility will not be examined further in the present analysis.

Considering together the comparisons for the three ratios, a suggestive picture emerges, ignoring destruction processes, in which protons below 30 MeV could account for essentially all the production of the light elements, conceivably within the context of a single mechanism. The Be abundances present no significant problem for such a model, because almost no Be is produced by protons of energy below 25 MeV, and the small observed amount (B/Be ~ 400 in the solar system[32]) can be attributed to small fluxes of higher-energy protons, to α particles, or to proton reactions with ^{13}C. It may be further noted that the attempt to fit these ratios with proton spectra characterized by a power law in kinetic energy ($E^{-\gamma}$), which has been a common form of parametrization for spectra concentrated at low energies, is unsuccessful largely because of the excessive production of ^{11}B from ^{14}N for $\gamma > 2$.

The possible role of α particles in light element production can also be discussed in the context of low-energy reactions, again ignoring destruction processes. If the B/Li ratio has the high CCG value, α particles above about 40 MeV would play little role, because of the large Li yields from the reactions ^{4}He$(\alpha, p)^7$Li and ^{4}He$(\alpha, d)^6$Li, with thresholds at α-particle energies of 34.7 and 44.7 MeV, respectively. It is to be noted that the abundance of ^{4}He far exceeds that of the CNO nuclei in any commonly hypothesized environment for light element production, and the cross sections for these ^{4}He + ^{4}He reactions are very substantial.[37] One can similarly exclude a large role for α particles at lower energies because α particles in the 20–40-MeV region have cross sections for ^{10}B production from ^{14}N which exceed the cross sections for ^{6}Li production by only a factor of 2 to 5, while the CCG abundance ratio is approximately 19. Nevertheless, a small contribution from α particles can be envisaged. Its most prominent effect would be to enhance the ^{6}Li yield and thus permit descriptions of light element production in which the dominant production mode involves reactions of protons below 20 MeV on ^{14}N and where the 7/6 ratio is held to reasonable levels by α-particle reactions on ^{14}N. If, on the other hand, the CCG B/Li ratio is too high, then a much more important role may be played by α particles, as could also be the case were the possibility of preferential destruction of Li is included. Viewed from another standpoint, the role of α particles is linked to the character of the particle distributions. If the α-particle flux is $\frac{1}{10}$ that of the proton flux at the same energy per nucleon, then a large contribution from α-particle reactions would appear to be likely in processes dominated by low-energy reactions. However, if the proton and α-particle fluxes are to be compared at the same energy, then α-particle reactions may be unimportant.

It is concluded that arguments based on cross-section systematics alone cannot at this time exclude the possibility that the light elements LiBeB are produced by a single mechanism, and that this mechanism is dominated by proton reactions occurring at energies below 30, or even 20, MeV. The hypothesis of a single *proton* dominated mechanism depends heavily on the validity of a high B/Li ratio because for proton reactions on CNO the B production cross sections exceed the Li cross sections for each of the targets (at the lower energies as well as up to 400 MeV[38]). A lower B/Li ratio could possibly be explained by considering α-particle reactions, as discussed above. More generally, whether the simple sort of description considered here will eventually prove viable, with or without α particles, will depend upon whether

environments can be found which provide the necessary low-energy particle spectra and in which the LiBeB abundances are not greatly modified by subsequent destruction processes.

ACKNOWLEDGMENTS

We wish to thank Dr. J. M. Cameron for help in the initial stages of the activation measurements and Dr. P. A. Russo for assistance during data taking. Informative discussions with Dr. R. I. Epstein and Dr. B. M. Tinsley are also acknowledged.

---

*Work supported in part by the U.S. Atomic Energy Commission.

†Present address: Department of Physics, University of North Carolina, Chapel Hill, North Carolina 27514.

[1]W. A. Fowler, G. R. Burbidge, and E. M. Burbidge, Astrophys. J. Suppl. 2, 167 (1955); E. M. Burbidge, G. R. Burbidge, W. A. Fowler, and F. Hoyle, Rev. Mod. Phys. 29, 547 (1957).

[2]R. Bernas, E. Gradsztajn, H. Reeves, and E. Schatzman, Ann. Phys. (N. Y.) 44, 426 (1967).

[3]H. Reeves, W. A. Fowler, and F. Hoyle, Nature 226, 727 (1970).

[4]M. Meneguzzi, J. Audouze, and H. Reeves, Astron. and Astrophys. 15, 337 (1971).

[5]H. E. Mitler, Astrophys. and Space Sci. 17, 186 (1972).

[6]H. Reeves, J. Audouze, W. A. Fowler, and D. N. Schramm, Astrophys. J. 179, 909 (1973).

[7]A. G. W. Cameron, S. A. Colgate, and L. Grossman, Nature 243, 204 (1973).

[8]J. Audouze and J. W. Truran, Astrophys. J. 182, 839 (1973).

[9]S. A. Colgate, to be published.

[10]R. V. Wagoner, Astrophys. J. 179, 343 (1973).

[11]A. G. W. Cameron and W. A. Fowler, Astrophys. J. 164, 111 (1971); J. M. Scalo and R. K. Ulrich, *ibid.* 183, 151 (1973); I. J. Sackman, R. L. Smith, and K. Despain, to be published.

[12]J. W. Truran and A. G. W. Cameron, Astrophys. and Space Sci. 14, 179 (1971).

[13]H. Reeves, On the Origin of the Light Elements, report, 1973 (to be published).

[14]A fuller description of this work and the experimental procedure is given in W. W. Jacobs, Ph.D. thesis, University of Washington, 1974 (unpublished).

[15]M. Epherre and C. Seide, Phys. Rev. C 3, 2167 (1971).

[16]H. Laumer, S. M. Austin, L. M. Panggabean, and C. N. Davids, Phys. Rev. C 8, 483 (1973).

[17]D. W. Storm *et al.*, Nuclear Physics Laboratory Annual Report, University of Washington, 1968 (unpublished), p. 124.

[18]E. A. Silverstein, Nucl. Instrum. Methods 4, 53 (1959).

[19]N. Jarmie, J. H. Jett, J. L. Detch, Jr., and R. L. Hutson, Phys. Rev. C 3, 10 (1971).

[20]H. Fuchs and K. H. Lindenberger, Nucl. Instrum. Methods 7, 219 (1960); J. B. Cumming, A. M. Poskanzer, and J. Hudis, Phys. Rev. Lett. 6, 484 (1961); J. B. Cumming, J. Hudis, A. M. Poskanzer, and S. Kaufman, Phys. Rev. 128, 2392 (1962); D. F. Measday, Nucl. Phys. 78, 476 (1966).

[21]T. Ericson and T. Mayer-Kuckuk, Annu. Rev. Nucl. Sci. 16, 183 (1966).

[22]F. Ajzenberg-Selove, Nucl. Phys. A152, 1 (1970).

[23]H. R. Weller, Phys. Lett. 30B, 409 (1969); P. N. Shrivastava, F. Boreli, and B. B. Kinsey, Phys. Rev. 169, 842 (1968); G. A. Huttlin and A. A. Rollefson, Phys. Rev. C 9, 576 (1974).

[24]J. G. V. Taylor and J. S. Merritt, Can. J. Phys. 40, 926 (1962).

[25]R. L. Heath, Atomic Energy Commission Research and Development Report No. IDO-16880-1, August, 1964 (unpublished), 2nd ed., Vol. I.

[26]D. J. Johnson and M. A. Waggoner, Phys. Rev. C 2, 41 (1970).

[27]R. I. Epstein, D. N. Schramm, and W. D. Arnett, Program of the Meeting of the Division of Cosmic Physics, American Physical Society, Tucson, Arizona, 1973 (unpublished).

[28]See, for example, Refs. 3, 4, 6, 7, and 8.

[29]D. C. Morton, J. F. Drake, E. G. Jenkins, J. B. Rogerson, L. Spitzer, and D. G. York, Astrophys. J. 181, L103 (1973).

[30]J. Audouze, J. Lequeux, and H. Reeves, Astron. and Astrophys. 28, 85 (1973).

[31]A. M. Boesgaard and W. D. Heacox, Astrophys. J. 185, L27 (1973).

[32]A. G. W. Cameron, Space Sci. Rev. 15, 121 (1974).

[33]M. Garcia-Munoz, G. M. Mason, and J. A. Simpson, Astrophys. J. 184, 967 (1973).

[34]C. N. Davids, H. Laumer, and S. M. Austin, Phys. Rev. C 1, 270 (1970).

[35]H. Laumer, S. M. Austin, and L. M. Panggabean, to be published.

[36]D. L. Oberg, D. Bodansky, D. D. Chamberlin, and W. W. Jacobs, Bull. Am. Phys. Soc. 17, 893 (1972).

[37]See, for example, Refs. 4 and 5.

[38]R. Silberberg and C. H. Tsao, Astrophys. J. Suppl. 25, 315 (1973).